Pergamon

Int. J. Heat Mass Transfer. Vol. 41, No. 14, pp. 2131–2142, 1998

Printed in Great Britain
0017-9310/98 $19.00+0.00

PII: S0017-9310(97)00349-9

The effect of tank geometry on thermally stratified sensible heat storage subject to low Reynolds number flows

P. C. EAMES† and B. NORTON

PROBE, Centre for Performance Research on the Built Environment, School of the Built Environment, University of Ulster, Newtownabbey BT37 0QB, Northern Ireland

(*Received* 28 *February* 1997 *and in final form* 6 *November* 1997)

Abstract—In a theoretical and experimental investigation into the thermal performance of stratified hot water stores, a transient three-dimensional finite-volume based model was validated by comparison with measured temperatures from a series of thirty-two experiments in which the inlet velocities, temperatures and initial store stratification profiles were varied. A parametric analysis ascertained the effect of inlet and outlet port locations on store performance for a range of operating conditions. The effects of finite volume size on predicted levels of entrainment and diffusion in the inlet region are reported. © 1998 Elsevier Science Ltd. All rights reserved.

1. INTRODUCTION

In direct thermosyphon [1] and 'low flow' [2] solar water heaters, the flow regimes are such that the water input to the storage tank is a low velocity laminar flow. Thermal stratification in the hot water storage tank is a determinant of overall system efficiency for many water heating systems. The thermocline within thermal water stores degrades due to:

- Convective entrainment; when the variable inlet fluid temperature is dissimilar to that of the fluid in the store in the region of inlet, the incoming fluid will rise or fall within the store entraining resident tank fluid.
- Heat-loss-driven natural convective flow resulting from heat transfer to ambient.
- Wall-conduction-driven natural convective flow resulting from thermal conduction via the store walls from warmer to cooler fluid.
- Heat diffusion due to the temperature gradient.
- Mixing arising from local turbulence at the inlet and outlet.

Minimisation and/or suppression of these mechanisms, will lead to a store that will remain stratified for longer periods of time, which will increase the total storage efficiency and exergy of withdrawn heated water.

The effects of wall conduction and heat loss from store to ambient combined with heat diffusion due to the temperature gradient have been extensively investigated both experimentally [3–6] and with the use of generally two-dimensional numerical models [5, 7, 8]. Thermocline degradation is dependent on both the thickness and thermal conductivity of store walls. Thermal conductivity similar to or less than that of water leads to degradation dominated by thermal diffusion effects. Increasing wall conductivity results in local convective currents being established within the store leading to a decrease in the time required for a uniform store temperature to be achieved. The effect of locating insulation on the interior and exterior of the store walls has been investigated [5], it was apparent that insulation located interior to the store, inhibits more effectively thermocline degradation both by reducing the effect of the conducting wall and the heat loss of the external environment. A numerical study [5], based on a two-dimensional finite difference model cast in cylindrical polar form enabled the effect of conducting walls and thermal insulation to be modelled for stores with rotational symmetry.

Theoretical investigations into forced convective flow through storage tanks have generally been based on simple one-dimensional models with correlations used to calculate rates of entrainment and mixing [9, 10]. Two-dimensional Cartesian and cylindrical coordinates have been employed [7, 8] to provide more detailed analysis. There are many experimental investigations [11, 12], a comprehensive review of which was published in 1989 [2]. Thermal stratification can be maintained by ensuring that velocities are low and thus essentially laminar flow is maintained, with little turbulent mixing at the inlet or outlet. A range of manifolding devices have been suggested consisting of baffle plates or perforated inlet tubes that better allow stratification to be maintained. The numerical models

† Author to whom correspondence should be addressed.

to date have been limited in that systems have been assumed to possess cylindrical symmetry or that two-dimensional wedge flow occurs. For many systems these assumptions are not appropriate and a full three-dimensional approach is required.

2. NUMERICAL MODELS

A range of numerical methods have been developed to model the thermofluid behaviour within systems. Recent advances in the finite volume method, in particular the movement to non-orthogonal coordinate systems combined with the use of non-staggered grids [13–16], have enabled complex geometries to be approximated accurately. The addition of the effective ability to use composite domains to subdivide problems and solve iteratively between the subdivisions enables large problems to be solved [17]. These developments however lead to an increased computational overhead which may prove prohibitive for some problems.

The basic formulation adopted in this work is based on the SIMPLE algorithm [18], due to its simplicity and the minimal matrix equation bandwidth that this method yields. A transient three-dimensional implementation employing a power law upwinding scheme and an orthogonal coordinate system, has been combined with the Bi-CGSTAB iterative equation solver [19]. Advantages of this approach are, the relatively low computer memory requirements, and the rapid convergence afforded by the Bi-CGSTAB algorithm when a good approximation to the solution is given, i.e. using the solution at time t, to calculate that at time $t+1$. For this work between 40 000 and 864 000 graded control volumes have been employed with a time step in the range 0.1–1 s. The Bi-CGSTAB algorithm is modified in that all the equations are normalised before solution, the convergence criteria adopted are $1\ e^{-8}$ for the momentum equations, $1\ e^{-6}$ for the pressure equations, $1\ e^{-10}$ for the temperature equations and for convergence at each time step the source term should be less than $2.5\ e^{-7}$.

3. FINITE VOLUME SIZE AND PREDICTED LEVELS OF ENTRAINMENT AND DIFFUSION

For a store with dimensions of $250 \times 250 \times 140$ mm, to investigate the effect of finite volume size on the predicted levels of entrainment and diffusion three simulations with finite volumes of side 2.5, 5 and 10 mm were undertaken. The store simulated was initially at a uniform temperature of 20°C, inlet and outlet ports of dimension 20×20 mm were located centrally on opposite store walls at heights of 150 mm and 100 mm, respectively. The inlet jet water temperature was 60°C and its velocity was 75 mm s^{-1}. The isotherm plots at a time of 60 s after the start of the simulations are presented in Fig. 1. Considering the three isothermal contour plots, A, through the vertical centre plane of the store, significant differences can be observed. The copper store walls are initially at 20°C, their thermal response lags that of the increasing fluid temperature due to their thermal mass and the rate of heat transfer from the fluid to them, leading to the sharp temperature gradient adjacent to the copper store walls evident in all three simulations. The contour plotting package used, employs linear interpolation between nodes explaining the thickness of the gradient zone in the simulation with the 10 mm dimension finite volumes. The general appearance of the mid plane isotherm plots for all three simulations can be seen to be similar. Due to the relative large size of the 10 mm dimension finite volumes, the fluid jet mixes, spreads and cools more relative to that predicted with the 5 and 2.5 mm dimension finite volumes, in addition greater thermal diffusion beneath the jet leads to the 22°C isotherm extending down the height of the tank further in this region. The use of 5 and 2.5 mm dimension finite volumes improves both temperature gradient resolution and also allows for finer scale structure of the temperature field to be revealed, this is particularly evident in the central region of the store above the inlet.

The isotherm plots for cross sections parallel to the store wall containing the inlet, at distances of 50 and 100 mm shown in B and C of Fig. 1, respectively, are generally similar. Section B shows clearly the inlet jet rising with little spreading in the y direction until the inlet jet fluid impinges on the upper store wall and recirculates. The predicted thermal diffusion below the level of the inlet is influenced strongly by the finite volume size, with 22°C contour further down the store for the 10 mm finite volumes. The 2.5 mm finite volume simulation reveals clearly a recirculating flow pattern. The hot inlet jet rises through the store entraining cooler fluid in its passage, on impinging with the top store wall, it flows along this surface spreading in the x and y directions. In the y direction it impinges on the flows down the vertical store wall, until buoyancy forces cause it to flow along the top of the cooler fluid layer below and then to rise again. At Section C the behaviour predicted is similar, however at this distance from the inlet the jet fluid is flowing along the top tank wall and is not evident in the main body of the tank fluid. The maximum temperature isotherms shown in Fig. 1C, for the 10, 5 and 2.5 mm finite volume simulations are 42, 46 and 48°C, clearly indicating the greater mixing/thermal diffusion predicted by the larger finite volumes. This would indicate for these small store simulations, small finite volumes are required to obtain accurate results, due to the high levels of recirculation and the large volume of the store affected directly by the inlet jet.

To model larger stores with uniform small finite volumes is at present a prohibitively expensive computational task. However using graded finite volumes, with dimensions of 5 mm adjacent to the store walls

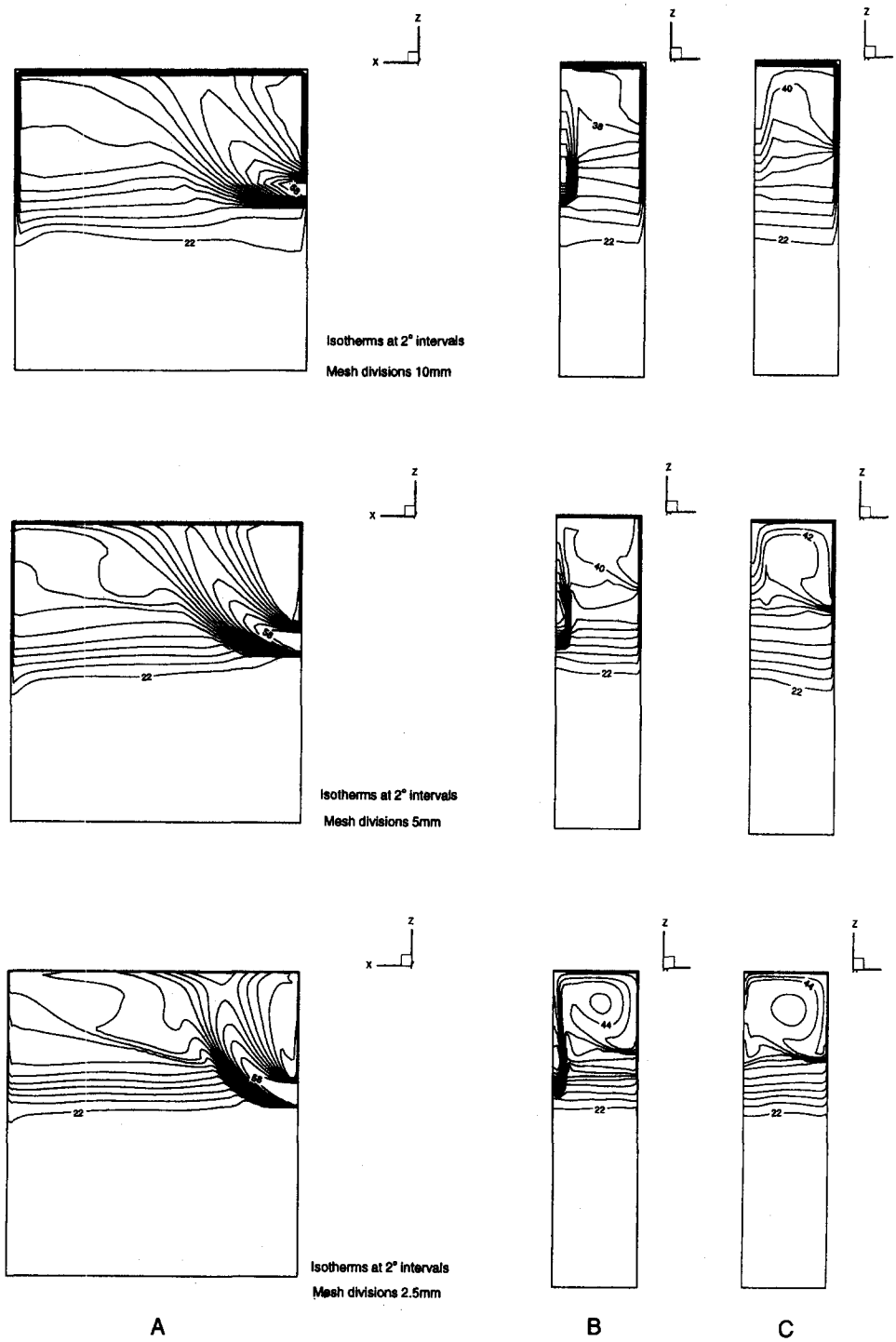

Fig. 1. Isotherm contour plots for three finite volume sizes at 60 s for a store of dimension 250 × 250 × 140 mm initially at a uniform 20°C temperature when subject to an inlet jet with a temperature of 60°C and a velocity of 75 mm s^{-1}. Inlet and outlet ports are sized 20 × 20 mm and are located centrally at heights of 150 mm and 100 mm on opposite vertical narrow store walls. A: Vertical central plane containing inlet and outlet ports. B: Vertical plane parallel to the store wall containing the inlet at a distance of 50 mm. C: Vertical plane parallel to the store wall containing the inlet at a distance of 100 mm.

and the store ports, increasing to 15 mm in the central store region excellent agreement with experimental observations was achieved.

4. EXPERIMENTAL VALIDATION

Six stores were employed; three 450 mm diameter copper cylinders with heights of 625, 900 and 1200 mm and wall thickness of 0.5 mm, and three purposely-built stores with transparent thermo-plastic walls, square cross section of side 450 mm and heights similar to those of the copper cylinders and wall thickness of 12 mm. A schematic diagram of the experimental facility developed is illustrated in Fig. 2. An immersion heater in a thermosyphon loop was employed to generate the initial thermocline within the store. The inlet jet velocity was controlled with a series of gate valves, a constant temperature for the inlet fluid was maintained by passing water heated in a constant head tank through two mixing tanks. An array of up to 44 copper/constantan thermocouples with an accuracy of $\pm 0.5°C$ were employed to monitor three-dimensional temperature evolution within the store. Additional thermocouples measured inlet, outlet, ambient and tank external wall temperatures. All inlets and outlets to the stores were of 22 mm diameter. Thirty two experimental tests were undertaken, with the inlet temperature ranging between 11 and 52°C, fluid inlet velocities in the range of 25–90 mm s^{-1} and various permutations of inlet and outlet port locations. Visualisation of flow was performed by introducing a dye into the constant head tank for the experiments with the transparent tanks.

From the experiments, if the inlet jet did not impinge directly on the store walls, either as a result of diffusion or buoyancy forces, for hot water stores with constant horizontal cross section, it was apparent that the store cross sectional geometry had little effect on the store stratification performance. Therefore assuming only store cross-sectional area and thus volume per unit height to be of importance, the cylindrical stores were for validation represented by stores with square cross section of equal area. Initial thermocline, inlet temperature, inlet velocity and ambient temperature for simulations of these stores were matched with those recorded experimentally. The dominant temperature gradients adjacent to the store walls within the store were in the vertical direction, to maintain equitable wall conduction paths, the thickness of the cylinder wall was scaled to account for the increase in store perimeter. The thickness of insulation and external heat loss coefficient were scaled as shown in Fig. 3 to account for the increase in store surface area and thus heat loss. For the transparent stores of square cross section all parameters were matched. A graded finite volume mesh was employed with dimensions of 5 mm adjacent to the store walls and the store ports, increasing to 15 mm in the central store region.

Typical examples of the level of agreement found are illustrated in Figs. 4 and 5. Figure 4 allows a comparison to be made between the thermocline

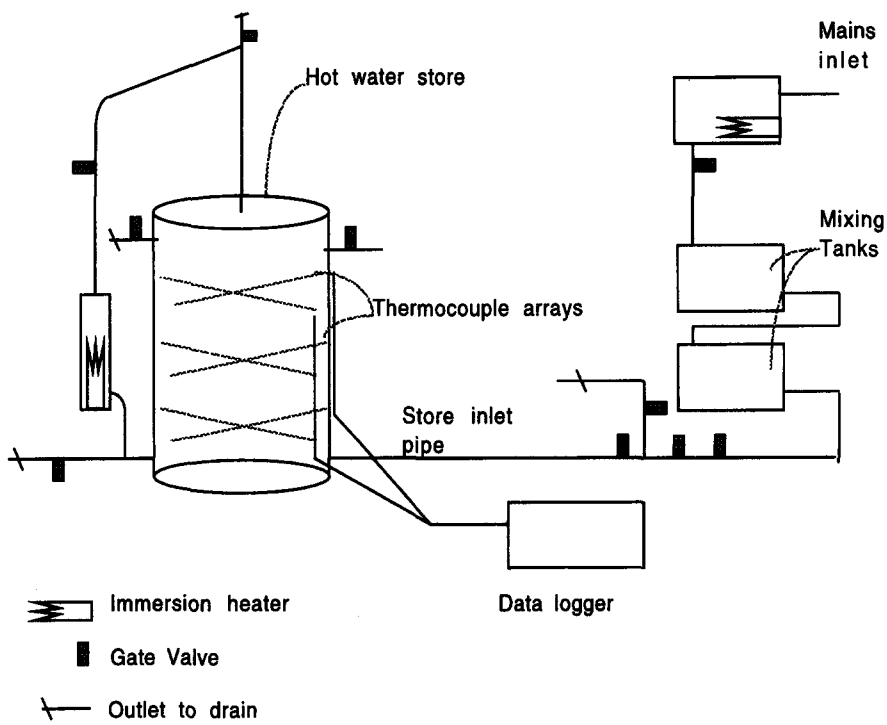

Fig. 2. A schematic diagram illustrating the experimental facility developed.

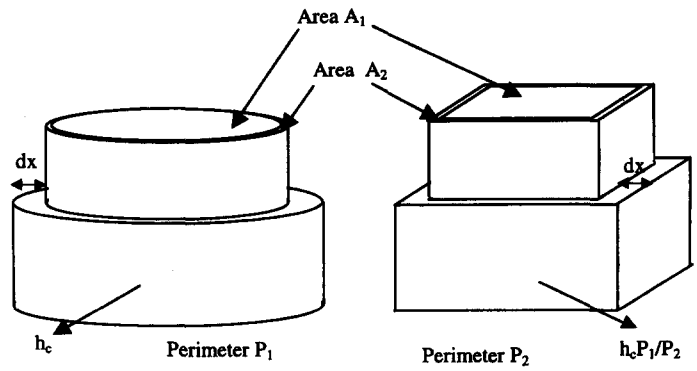

Area A_1	Store cross sectional area
Area A_2	Store wall cross sectional area
dx	Insulation thickness
Perimeter P_1	Outer Perimeter area for circular cross section store
Perimeter P_2	Outer Perimeter area for square cross section store
h_c	Convective heat transfer coefficient

Fig. 3. The scaling factors and geometrical conversions adopted to allow the simulation of stores with circular cross section by stores with square cross section.

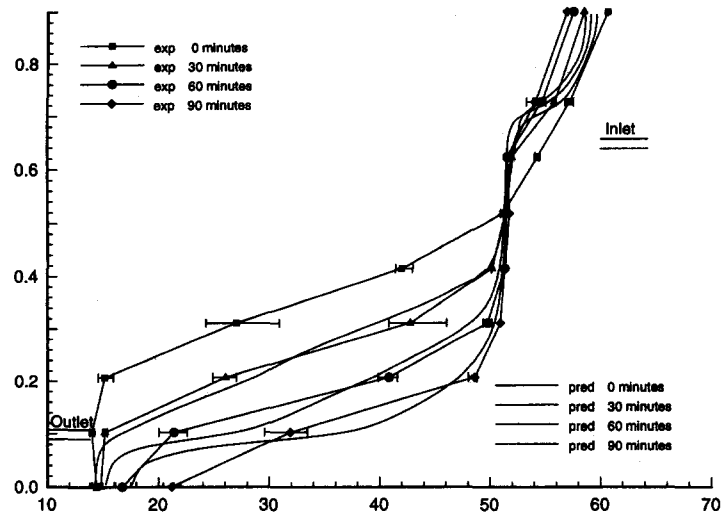

Fig. 4. Computed and experimentally determined thermoclines for a copper hot water store 450 mm diameter 900 mm tall, when subject to a laminar inlet jet with an average temperature of 51.8°C and velocity of 24 mm s^{-1}.

measured experimentally and that predicted by the model for the 900 mm tall copper cylinder. The evolving thermocline for the experimental data is drawn through the average of four temperatures measured at each height: additionally the maximum and minimum of the four temperatures measured at each height are plotted to give an indication of the temperature variation at each height for each given time. The predicted thermocline is constructed from the average temperature of all control volumes at each given height. The average fluid inlet temperature was 51.8°C, the average inlet fluid velocity was 24 mm s^{-1}. In the store region between the inlet and outlet the agreement is excellent. The measured temperature in the region above the inlet decreases more rapidly than predicted. There are several possible reasons for this:

- the model does not account for the 150 mm high upper domed upper surface of the cylinder, thus the thermal mass of the water is overestimated,

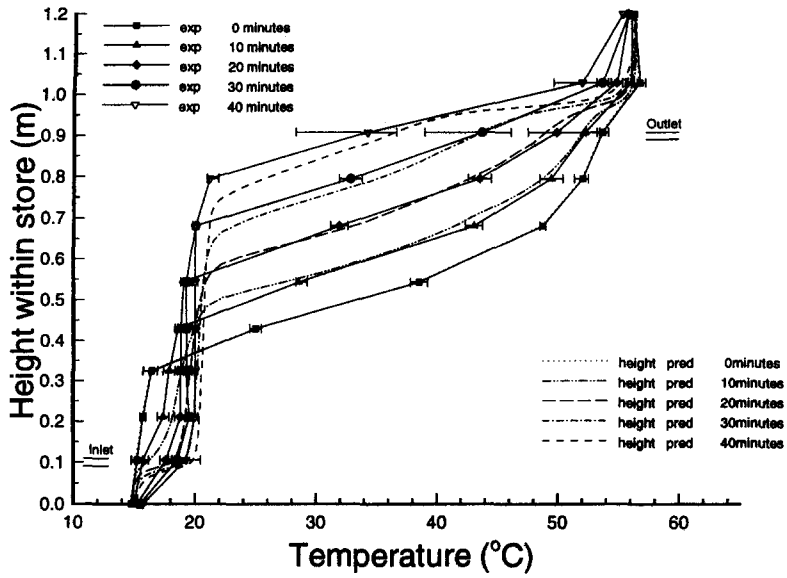

Fig. 5. Computed and experimentally determined thermoclines for a copper hot water store 450 mm diameter 1200 mm tall, when subject to a laminar inlet jet with an average temperature of 23°C and velocity of 63 mm s^{-1}.

- the heat loss coefficient from the surface of the cylinder was underestimated,
- the pipework at the top of the cylinder was acting like a cooling fin,
- the temperature at the top of the store was measured by attaching a thermocouple to the exterior surface of the cylinder. (Due to the high thermal conductivity of the thin copper store wall, the exterior wall surface temperature was taken to be similar to that of the water within the store adjacent to this surface.)

Below the outlet the simulation predicts a smaller temperature rise in response to essentially conduction from the water above; this is due to the larger volume of water below the outlet in the simulation compared to that in the experiment due to the domed cylinder base, additionally a sacrificial anode in the base of the tank may have lead to enhanced conduction.

The excellent agreement obtained between model and experiment for the 1200 mm tall copper cylinder can be seen in Fig. 5. The only slight discrepancy is above the outlet, the possible reasons for this are as listed previously.

5. PARAMETRIC ANALYSIS

The model was employed to investigate the effects of convective flow through two stores the dimensions of which are given in Table 1, with two different inlet port locations as illustrated in Fig. 6. Symmetry conditions were utilised with half of the store simulated. The duration of each simulation was selected to be that required for one complete volume change of the store to take place. The stores modelled had 1 mm thick copper walls insulated with a 6 mm thickness of insulant with a thermal conductivity of 0.035 W m^{-1} K^{-1}. To effectively remove the effects of heat loss to the ambient environment, and isolate the simulated effects to mixing induced by the flow through the tank and that due to conduction in the walls, the heat transfer coefficient from the external insulant surface to the ambient environment was set to (essentially) zero.

Inlet and outlet ports were located in opposite sides of the store, with a distance between their centre line and the top and base of the store such that for both stores equivalent volumes of water are above/below the port centre lines. In the flow initiation phase for these simulations the time step was increased from 0.1–1 s over a simulated time period of thirty seconds.

5.1. *Store charging efficiency*

The stores were initially at a uniform datum temperature of 20°C. Inlet jets with temperatures of 60°C and flow velocities of 50, 75 and 100 mm s^{-1} through a port of area 0.0004 m^2, corresponding to Reynolds numbers at inlet of, 1980, 1485 and 990 were simulated. The simulation times were 4050, 3038 and 2025 s, respectively. Figure 7 shows the predicted evolution of the fluid temperature at the outlet from the store, for these simulations, normalised with respect to the time required for one complete store volume change.

For the simulated thermal stores, with their outlets one ninth of the way up the store wall, if perfect charging occurred with no mixing of inlet fluid with resident store fluid, and no thermal diffusion taking

Table 1. Store dimensions and port locations

	Height (m)	Width (m)	Length (m)	Inlet heights (m)	Outlet heights (m)
Store A1	0.9	0.3	0.3	0.8	0.1
Store A2	0.9	0.3	0.3	0.45	0.1
Store B1	0.3	0.3	0.9	0.2667	0.033
Store B2	0.3	0.3	0.9	0.15	0.033

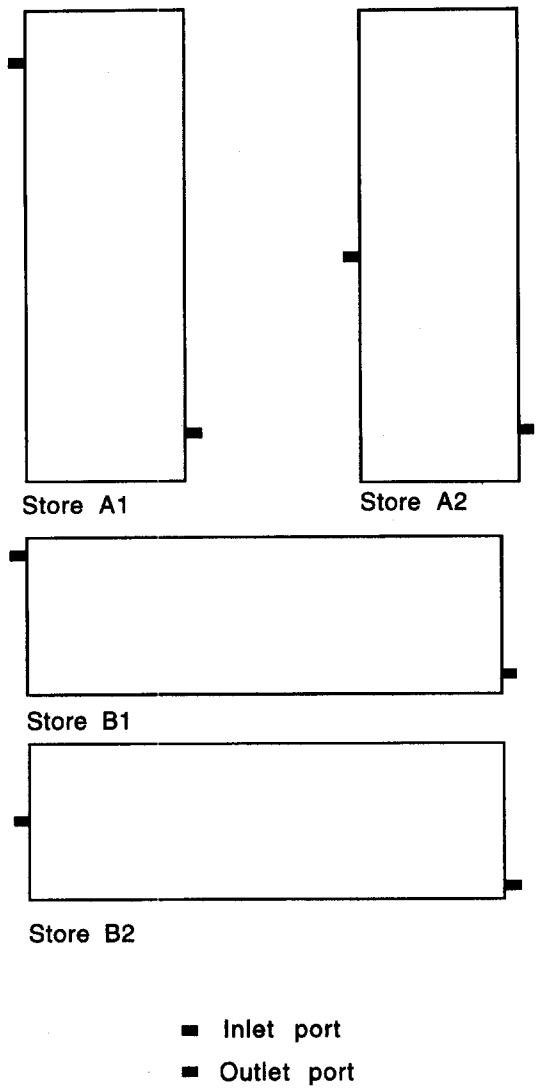

Fig. 6. A schematic illustrating the aspect ratios of stores simulated and the location of inlet and outlet ports. All stores are 300 mm wide.

place, a step change in the outlet fluid temperature from 20–60°C would take place at a normalised time of 0.88. The simulation which approaches this most accurately charges the most efficiently. By this criterion it can be seen from Fig. 7 that store A1 with an inlet velocity of 100 mm s^{-1} charges most efficiently, this is also shown by the average outlet temperature for this simulation being the lowest predicted. From the simulations performed over the 'normalised time' the most inefficient charging for all four store configurations occurred for a fluid inlet velocity of 75 mm s^{-1}, this was due to the compound effect of mixing and thermal diffusion, fluid mixing increased compared to the fluid inlet velocity of 50 mm s^{-1} and due to the longer simulated time, thermal diffusion increased compared to that for the fluid inlet velocity of 100 mm s^{-1}. For all inlet velocities stores A1 and B1 with inlets near the top charged more efficiently, A1 having slightly lower average outlet temperatures is the most efficient. Store B2 for all inlet velocities has lower average outlet temperatures than A2, this indicates that B2 is charging more efficiently, this is however a result of a less effective dead zone beneath the outlet.

5.2. *Thermocline development*

The thermocline development for the simulated stores with an inlet flow velocity of 75 mm s^{-1} and an inlet temperature of 60°C into a store initially at a uniform temperature of 20°C are shown in Fig. 8. The thermocline profiles for stores A1 and B1 are similar, however two important differences are that, a larger volume at the top of store A1 attains a temperature above 59°C by 1800 s, and greater thermal diffusion over the larger horizontal surface area leads to an increase in temperature of 3°C at the base of store B1, this also accounts for the smaller gradient of the thermocline in store B1. With inlets half way up the store walls B2 and A2 perform in a markedly different fashion, the jet in travelling through half the height of the store, entrains fluid and mixes more effectively, this leads to a smaller gradient of the thermocline and a less rapid rise in the temperature of water at the top of the store. After 1800 s maximum temperatures of only 50°C have been attained, the top half of store A2 being at a more uniform temperature than B2. A very sharp thermal gradient in store A2 at the height of the outlet exists with the temperature of the fluid in the volume below this rising only slowly by thermal diffusion, giving rise to an effective dead zone. In store B2 due to the smaller vertical distance between the outlet and the base of the tank and the increased horizontal cross-sectional area thermal diffusion effects are larger and this dead zone is less pronounced with temperatures approaching 26°C. This effect leads to the total energy retained within store B2, being larger than that in A2, leading to the consequently better charging reported in Section 4.1.

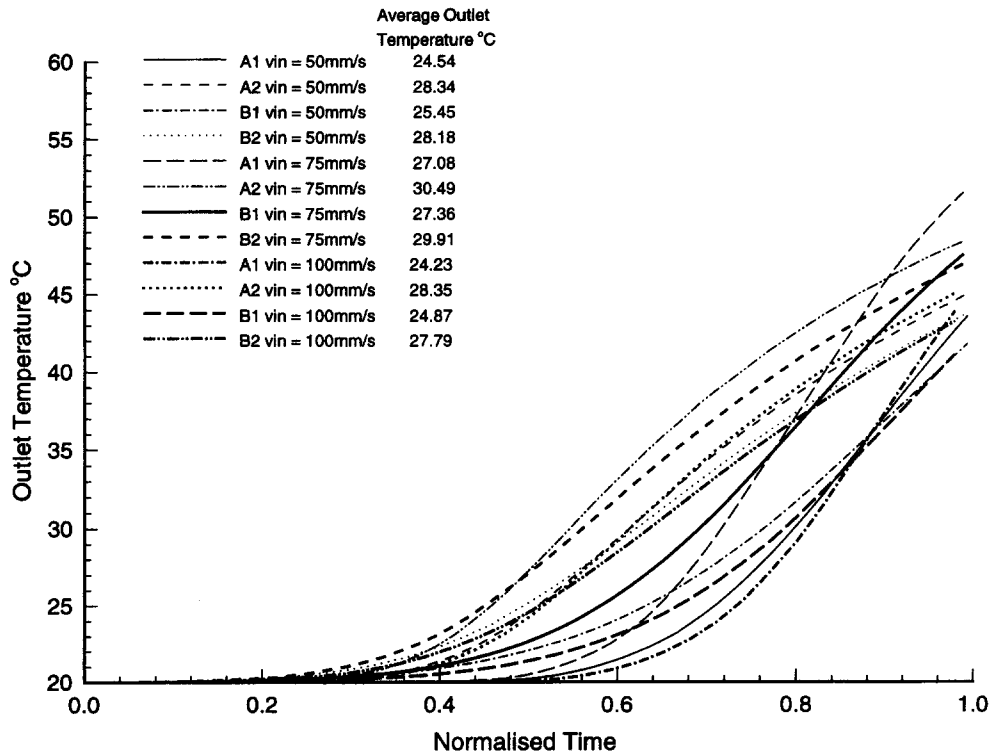

Fig. 7. The evolution of store fluid outlet temperature with normalised time (normalised time = simulation time/time required for flow through of one store volume).

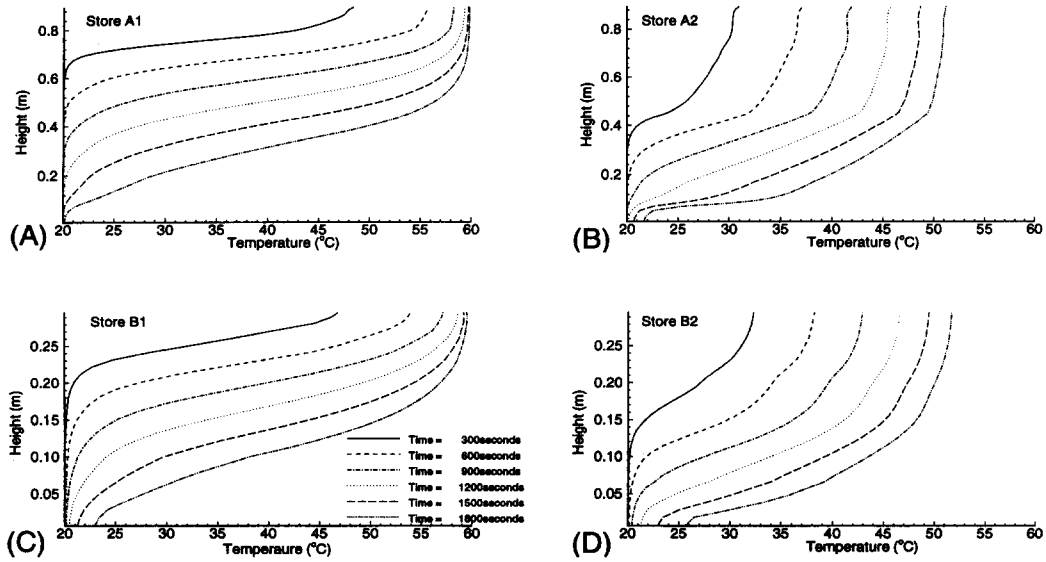

Fig. 8. Thermocline development for stores initially at a uniform temperature of 20°C, when subject to inlet jet flows with velocities of 75 mm s^{-1} and temperatures of 60°C: (A) store A1, (B) store A2, (C) store B1 and (D) store B2.

5.3. *Stratified store with variable inlet temperature*

For a 75 mm s^{-1} inlet velocity and a store with an initially stratified thermocline as illustrated at time 0 in Fig. 9, simulations of 5400 s were undertaken. A linear increase in the inlet temperature from 20–70°C was imposed over the first 2700 s, followed by a linear decrease to 30°C over the remaining simulation time. The thermocline evolution for these simulations are illustrated in Figs. 9 and 10.

Figure 9 illustrates clearly for stores A1 and B1 the rapid de-stratification that results when a cold inlet jet enters into the top hot layer of a thermally stratified store. All store fluid excluding that within the regions above the inlet and below the outlet, is by 1200 s in the temperature range 42–44°C. The temperature of the inlet fluid exceeds that of the resident store fluid at the height of the inlet between 1200 and 1500 s, and leads to a subsequent re-establishment of a thermal gradient within the store. Greater thermal conduction into the dead zones above the inlet and below the outlet for store B1 leads to significant temperature differences compared to that in the similar regions of store A1. The base of store B1 attains a temperature of 42.5°C at 2400 s compared to 30.7°C in store A1. For stores A2 and B2, with their inlets at the mid-height of the stores the fluid temperature in the top third of the stores is maintained. A very steep temperature gradient is initially established in store A2, with at 900 s the fluid above the inlet above 59°C, that between the inlet and outlet at 36°C, and a decrease to a base temperature of 22°C. After this time the inlet fluid temperature is increasing above that of the resident store fluid below the inlet, leading to the establishment of a linear temperature gradient region, which extends from the height of the inlet to that of the outlet. The thermocline of store B2 follows a similar general evolution to store A2, however greater levels of conduction heat transfer lead to shallower thermal gradients, and the store fluid temperature above the inlet and below the outlet decreasing and increasing more, respectively.

Figure 10 show the thermocline evolution for the four stores from 2700–5100 s, the period over which the inlet fluid temperature is reducing. The gradient region established in store A1 in the previous 2700 s is effectively destroyed, at 5100 s the fluid in the store is at a uniform 53°C, except for the small amount of fluid above the inlet. Store B1 performs in a similar fashion however greater thermal conduction effects lead to reduced temperature gradients, particularly above the inlet and below the outlet. In store A2 at 5100 s, the top half of the store is at a temperature above 60°C, with the bottom half at a uniform 50°C, a steep gradient zone exists in the store at the inlet height. In store B2 at 5100 s, the top third of the store is at a temperature above 60°C, with the bottom third

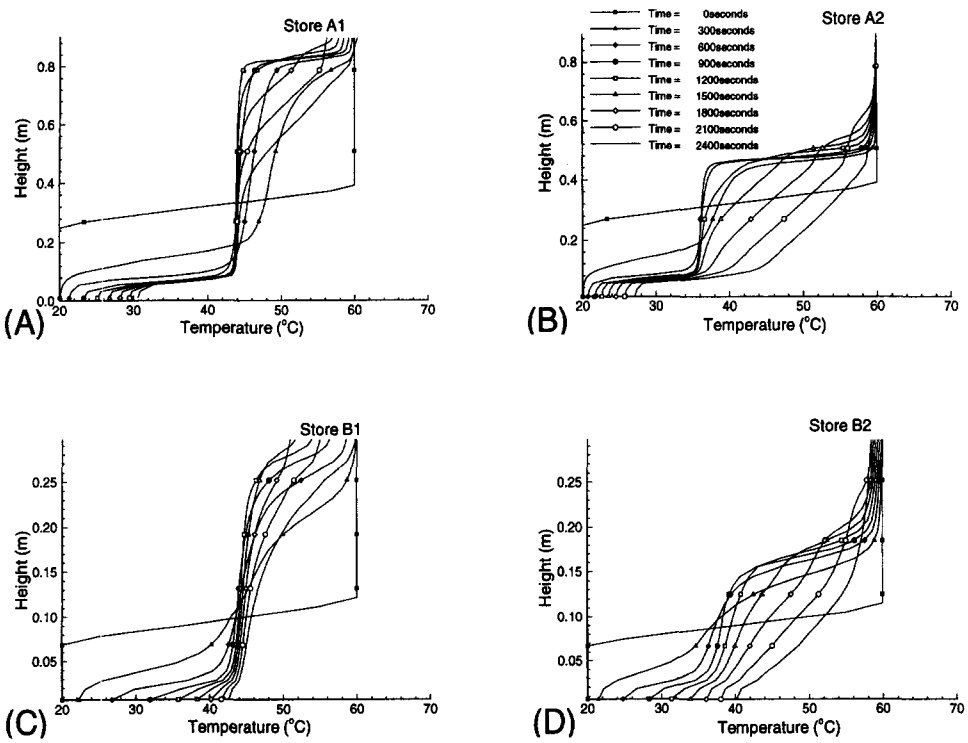

Fig. 9. Thermocline development for stores initially stratified as illustrated at time 0, for an inlet jet with velocity of 75 mm s^{-1} and temperature increasing linearly from 20–70°C over 2700 s, then linearly decreasing to 30°C over the following 2700 s. Thermoclines illustrated from 0–2400 s at 300 s intervals: (A) store A1, (B) store A2, (C) store B1 and (D) store B2.

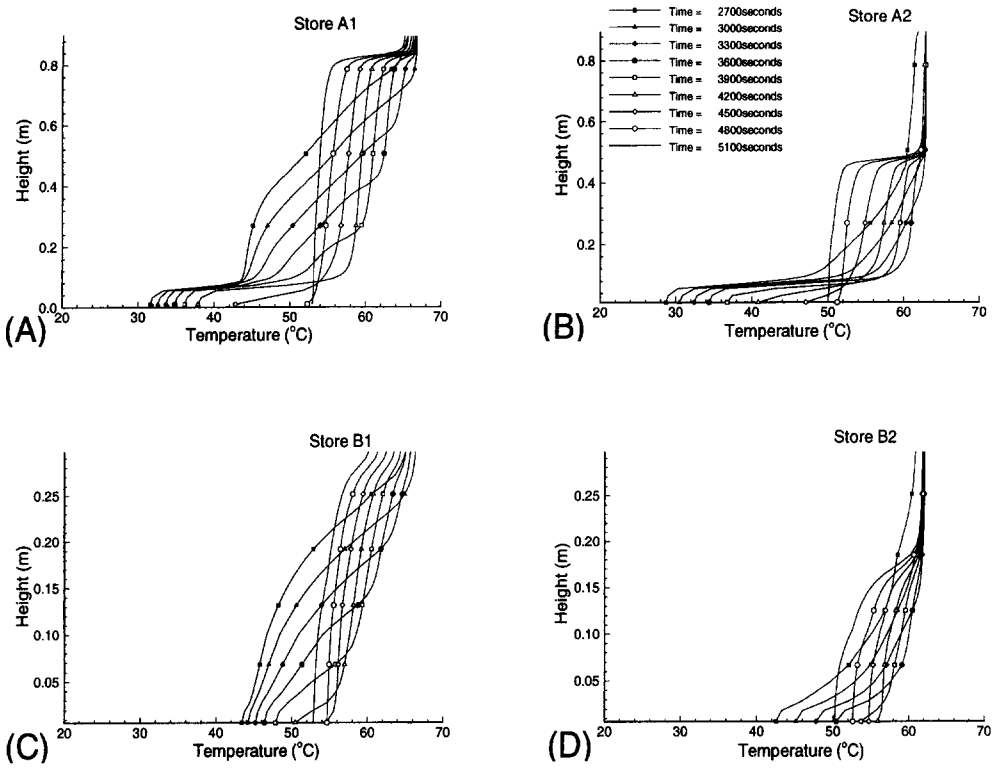

Fig. 10. Thermocline development for stores initially stratified as illustrated at time 0 in Fig. 9, for an inlet jet with velocity of 75 mm s^{-1} and temperature increasing linearly from 20–70°C over 2700 s, then linearly decreasing to 30°C over the following 2700 s. Thermoclines illustrated from 2700–5100 s at 300 s intervals: (A) store A1, (B) store A2, (C) store B1 and (D) store B2.

between 50 and 51°C, with a shallow thermal gradient zone in the middle third. Stores B2 and A2 can deliver significant volumes of water at higher temperatures than stores A1 and B1 at 5100 s, the exergy of water withdrawn from the tops of the stores B2 and A2 will thus, be greater.

The instantaneous outlet temperature and the average outlet temperature development for the four stores and the imposed inlet temperature are shown in Fig. 11. The outlet temperature is a direct measure of the rate of energy leaving the system, the average outlet temperature is a cumulative measure of the energy leaving the system and thus can be used to grade store efficiency. It is evident that at 400 s store A1 is losing energy at the greatest rate, this is a consequence of the cool inlet jet falling due to buoyancy effects, traversing the hot fluid below the inlet and causing significant mixing. Stores A1 and B1 initially lose more energy than they receive not regaining their initial energy content until after 1800 s, this is indicated by the crossing of the average outlet temperature lines with the average inlet temperature line. By 4000 s although the rate of heat loss from the four stores has varied greatly the cumulative value is such that the difference in average outlet temperature is less than 1°C.

At 5400 s the average temperature of water leaving the stores varies by less than 1.14°C, being for A1, A2, B1, B2, respectively, 45.13, 44.14, 45.27, 44.85°C. This corresponds to 775 kJ or a difference in average store temperature of less than 2.3°C, it is evident that the inlet port location for the above simulations has only a small effect on the store efficiency.

6. COMPARISON WITH ONE-DIMENSIONAL MODELS

In general it is not possible for an energy system designer to utilise detailed transient three-dimensional models, however simple one-dimensional models have been developed for this purpose. A comparison of predictions made with the transient three-dimensional model described herein and two simple one-dimensional models, revealed that for store-charging the three-dimensional model predicts charging efficiency between that of the two forms of one-dimensional model, these are:

- inlet fluid passes through the store without mixing being deposited in the store at a height at which the tank fluid is of equal temperature and
- inlet fluid mixes with each successive layer until no temperature inversion exist.

The first form of one-dimensional model predicts both

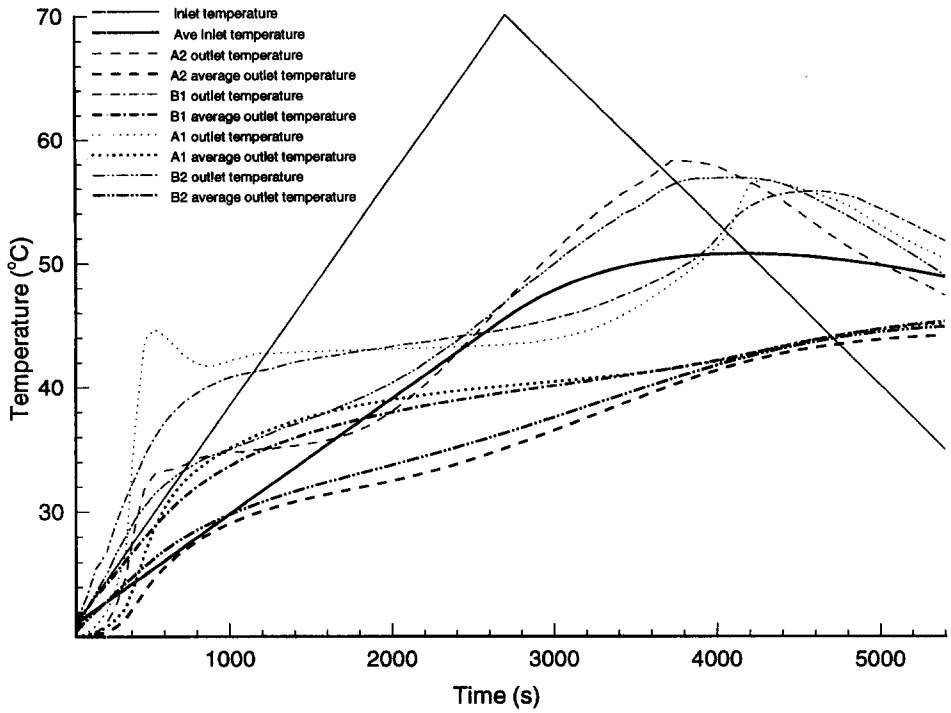

Fig. 11. The evolution of fluid outlet temperature and average outlet temperature for stores A1, B1, A2 and B2 initially stratified as illustrated at time 0 in Fig. 9, for an inlet jet with velocity 75 mm s^{-1} and temperature increasing linearly from 20–70°C over 2700 s, then linearly decreasing to 30°C over the following 2700 s.

the highest levels of stored energy and the maximum temperature of the three models. Due to prediction of convective mixing resulting from conduction in the store walls and heat loss from the store walls to ambient for periods of no flow, the three-dimensional model predicts faster degradation of the store thermocline than either one-dimensional approach. By increasing the thermal conductivity in the one-dimensional models, it is possible however to simulate the faster levels of degradation.

7. CONCLUSIONS

From the experimental and numerical studies undertaken and reported a range of conclusions can be drawn:

(1) To obtain converged solutions independent of finite volume size for fluid inlet velocities of 75 mm s^{-1} for stores of size 250 × 250 × 140 mm, with inlet and outlet ports of size 20 × 20 mm, and an inlet fluid temperature 40°C greater than that of the resident store fluid initially, finite volumes of side less than 5 mm are required.

(2) Increased levels of both thermal diffusion and entrainment are predicted for finite volumes of side 10 mm compared to those for finite volumes of side 5 and 2.5 mm.

(3) Graded finite volumes concentrated in areas of inlet and outlet and adjacent to store boundaries can produce similar results to uniform small finite volumes.

(4) Graded finite volumes, with dimensions of 5 mm adjacent to the store walls and the store ports, increasing to 15 mm in the central store region gave excellent agreement with experimental results for laminar inlet jets into thermally stratified stores.

(5) From experiments with stores of constant square cross section of side 450 mm, and constant circular cross section of 450 mm diameter it was found that, when subject to low velocity inlet jets, store cross sectional geometries had little influence on the thermocline development.

(6) Simulations undertaken for stores with aspect ratios (height to width) of 3:1 (tall) and 1:3 (short), with inlet ports either one ninth or half way down the store side revealed that store charging is performed more efficiently for tall stores, with the inlet port near the top of the store.

(7) For the simulated case with a steady inlet flow velocity of 75 mm s^{-1} and the inlet jet temperature increasing from initially 20–70°C and then back down to 30°C over a 90 min period only small differences in performance were predicted, the tall store with the inlet half way down the store side performing best.

(8) It was evident from simulations that a single inlet port with variable inlet temperature jet lead to

poor store charging performance, enhanced performance could be achieved by having a range of ports at different heights, the inlet fluid entering the store at the height at which the resident store fluid temperature most closely matches the inlet fluid temperature.

(9) A comparison with two simple one-dimensional models revealed that they either over or underestimated fluid entrainment and mixing, and during times of no flow underestimated the rate at which the thermocline degraded due to convective mixing resulting from both heat loss from and conduction within the store walls.

Acknowledgement—This work was supported by the Engineering and Physical Sciences Research Council, Swindon, U.K.

REFERENCES

1. Hobson, P. A. and Norton, B., Verified performance simulation model of direct thermosyphon solar-energy water heaters. *ASME Journal of Solar Energy Engineering*, 1988, **110,** 282–292.
2. Hollands, K. G. T. and Lightstone, M. F., A review of low flow, stratified-tank solar water heating systems. *Solar Energy*, 1989, **43,** 97–106.
3. Miller, C. W., The effect of a conducting wall on a stratified fluid in a cylinder. *Proceedings of the AIAA 12th Thermophysics Conference*, Albuquerque, U.S.A., 1977, pp. 1–9.
4. Sherman, C., Wood, B. D. and Masson, J., Effect of vertical wall conduction on temperature relaxation in thermally stratified liquid thermal storage tanks. *Proceedings of ISES Conference*, Atlanta, U.S.A., 1979, pp. 591–595.
5. Shyu, R. J., Lin, J. Y. and Fang, L. J., Thermal analysis of stratified storage tanks. *ASME Journal of Solar Energy Engineering*, 1989, **111,** 54–61.
6. Satanaryana Murthy, S., Nelson, J. E. B. and Sitharama Rao, T. L., Effect of wall conductivity on thermal stratification. *Solar Energy*, 1992, **49,** 273–277.
7. Parrini, F., Vitale, S. and Castellano, L., Rational analysis of mass, momentum and heat transfer phenomena in liquid storage tanks under realistic operating conditions: 2. Application to a feasibility study. *Solar Energy*, 1992, **49,** 95–106.
8. Parrini, F., Vitale, S., Alabiso, M. and Castellano, L., Rational analysis of mass momentum and heat transfer phenomena in liquid storage tanks under realistic operating conditions: 1. Basic formulation. *Solar Energy*, 1992, **49,** 87–94.
9. Kleinbach, E. M., Beckman, W. A. and Klein, S. A., Performance study of one-dimensional models for stratified thermal storage tanks. *Solar Energy*, 1993, **50,** 155–166.
10. Yoo, H. and Pak, E. T., A theoretical model of the charging process for stratified thermal storage tanks. *Solar Energy*, 1993, **51,** 513–520.
11. Lavan, Z. and Thompson, J., Experimental study of thermally stratified hot water storage tanks. *Solar Energy*, 1977, **19,** 519–524.
12. Mavros, R., Belessiotis, V. and Haralambopoulos, D., Stratified energy storage vessels: characterisation of performance and modelling of mixing behaviour. *Solar Energy*, 1994, **52,** 327–336.
13. Melaaen, M. C., Calculation of fluid flows with staggered and nonstaggered curvilinear nonorthagonal grids—the theory. *Numerical Heat Transfer, B*, 1992, **21,** 1–19.
14. Melaaen, M. C., Calculation of fluid flows with staggered and nonstaggered curvilinear nonorthagonal grids—a comparison. *Numerical Heat Transfer, B*, 1992, **21,** 21–39.
15. Melaaen, M. C., Nonstaggered calculation of laminar and turbulent flows using curvilinear nonorthagonal coordinates. *Numerical Heat Transfer, A*, 1993, **24,** 375–392.
16. Zhang, Y., Street, R. L. and Koseff, J. R., A non-staggered grid, fractional step method for time-dependent incompressible Navier–Stokes equations in curvilinear coordinates. *Journal of Computational Physics*, 1994, **114,** 18–33.
17. Zhang, Y. and Street, R. L., A composite multigrid method for calculating unsteady incompressible flows in geometrically complex domains. *International Journal for Numerical Methods in Fluids*, 1995, **20,** 341–361.
18. Patanker, S. V., *Numerical Heat Transfer and Fluid Flow*. Taylor and Francis, London, 1980.
19. Van der Vorst, H. A., Bi-CGSTAB: a fast smoothly converging variant of Bi-CG for the solution of nonsymmetric linear systems. *SIAM Journal of Scientific and Statistical Computing*, 1992, **13,** 631–644.